Evolution of Spin-Wave Excitations in Ferromagnetic Metallic Manganites

F. Ye,[1] Pengcheng Dai,[2,1,*] J. A. Fernandez-Baca,[1,2] Hao Sha,[3] J. W. Lynn,[4] H. Kawano-Furukawa,[5] Y. Tomioka,[6] Y. Tokura,[6,7] and Jiandi Zhang[3]

[1]*Center for Neutron Scattering, Oak Ridge National Laboratory, Oak Ridge, Tennessee 37831-6393, USA*
[2]*Department of Physics and Astronomy, The University of Tennessee, Knoxville, Tennessee 37996-1200, USA*
[3]*Department of Physics, Florida International University, Miami, Florida 33199, USA*
[4]*NIST Center for Neutron Research, Gaithersburg, Maryland 20899, USA*
[5]*Department of Physics, Ochanomizu University, Bunkyo-ku, Tokyo 112-8610, Japan*
[6]*Correlated Electron Research Center (CERC), Tsukuba 305-0046, Japan*
[7]*Department of Applied Physics, University of Tokyo, Tokyo 113-8656, Japan*

(Received 31 August 2005; published 30 January 2006)

Neutron scattering results are presented for spin-wave excitations of three ferromagnetic metallic $A_{1-x}A'_xMnO_3$ manganites (where A and A' are rare- and alkaline-earth-metal ions), which when combined with previous work elucidate the systematics of the interactions as a function of carrier concentration x, on-site disorder, and strength of the lattice distortion. The long-wavelength spin dynamics show only a very weak dependence across the series. The ratio of fourth to first neighbor exchange (J_4/J_1) that controls the zone boundary magnon softening changes systematically with x, but does not depend on the other parameters. None of the prevailing models can account for these behaviors.

DOI: 10.1103/PhysRevLett.96.047204 PACS numbers: 75.30.Ds, 61.12.−q, 71.30.+h

Determining the evolution of the elementary magnetic excitations in $A_{1-x}A'_xMnO_3$ (where A and A' are rare- and alkaline-earth-metal ions, respectively) is the first step in understanding the magnetic interactions in these doped perovskite manganites. According to the conventional double-exchange (DE) mechanism [1], the motion of charge carriers in the metallic state of $A_{1-x}A'_xMnO_3$ establishes a ferromagnetic (FM) interaction between spins on adjacent Mn^{3+} and Mn^{4+} sites. In strong Hund-coupling limit, the spin-wave excitations of a DE ferromagnet below the Curie temperature T_C can be described by a Heisenberg Hamiltonian with only the nearest-neighbor exchange coupling [2]. At the long-wavelength (small wave vector q), spin-wave stiffness D measures the average kinetic energy of charge carriers and therefore should increase with increasing x [2,3]. While spin dynamics of some manganites initially studied appeared to follow these predictions [4,5], later measurements revealed anomalous zone boundary magnon softening deviating from the nearest-neighbor Heisenberg Hamiltonian for other materials with $x \sim 0.3$ [6–10]. Three classes of models have been proposed to explain the origin of such deviations. The first is based on the DE mechanism, considering the effect of the on-site Coulomb repulsion [3] or the conducting electron band (e_g) filling dependence of the DE and superexchange interactions [11]. The second suggests that magnon-phonon coupling [8,12] or the effects of disorder on the spin excitations of DE systems [13] is the origin for the zone boundary magnon softening. Finally, quantum fluctuations of the planar $(x^2 - y^2)$-type orbital associated with the A-type antiferromagnetic (AFM) ordering may induce magnon softening as the precursor of such AFM order [14]. Although all these models appear to be reasonable in explaining the zone boundary magnon softening near $x = 0.3$, the lack of complete spin-wave dispersion data for $A_{1-x}A'_xMnO_3$ with $x < 0.3$ and $x > 0.4$ means that one cannot test the doping dependence of different mechanisms and, therefore, the origin of the magnon softening is still unsettled.

Very recently, Endoh *et al.* [15] measured spin-wave excitations in the FM phase of $Sm_{0.55}Sr_{0.45}MnO_3$ (SSMO45) and found that the dispersion can be described phenomenologically by the Heisenberg model with the nearest-neighbor (J_1) and fourth-nearest (J_4) neighbor exchange coupling (Fig. 1). By comparing the J_4/J_1 ratios, which measure the magnitude of the zone boundary magnon softening of SSMO45 with that of $Pr_{0.63}Sr_{0.37}MnO_3$ (PSMO37) [6] and $La_{1-x}Sr_xMnO_3$ ($x = 0.2, 0.3$; LSMO20, LSMO30) [5], the authors concluded that J_4/J_1 increases dramatically for $A_{1-x}A'_xMnO_3$ with $x > 0.3$. Since theoretical analysis based on the local density approximation + Hubbard U band calculations reveal that this doping dependence is consistent with the effect of rodlike $(3z^2 - r^2)$ orbital correlations, the authors argue that the observed zone boundary magnon softening in $A_{1-x}A'_xMnO_3$ is due to the $(3z^2 - r^2)$-type orbital fluctuations, in sharp contrast to all previous proposals [15].

In this Letter, we take an approach different from that of Endoh *et al.*, as we know that J_4/J_1 is nonzero for $x = 0.3$ manganites such as LSMO30 (Figs. 3 and 4) [16] and $La_{0.7}Ca_{0.3}MnO_3$ (LCMO30) [8], in contrast with the expectation of Refs. [5,15]. We decided to systematically analyze all existing spin-wave excitation data and take additional data in the FM metallic state of $A_{1-x}A'_xMnO_3$ at judicially selected x. We find that the low-q spin-wave stiffness D is insensitive to x while spin-wave excitations are systematically renormalized near the zone boundary with J_4/J_1 proportional to x. We also find that on-site

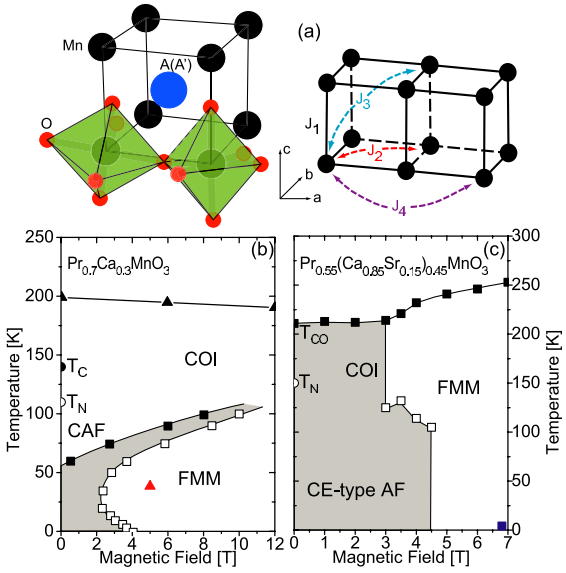

FIG. 1 (color online). (a) Crystal structure of $A_{1-x}A'_xMnO_3$ with magnetic exchange coupling indicated. (b) Phase diagram of $Pr_{0.7}Ca_{0.3}MnO_3$ in the T-H plane [19]. (c) Phase diagram of $Pr_{0.55}(Ca_{0.85}Sr_{0.15})_{0.45}MnO_3$ in the T-H plane from transport measurements. Our neutron experimental conditions are marked as the (red) upper triangle and the (blue) square in the phase diagrams.

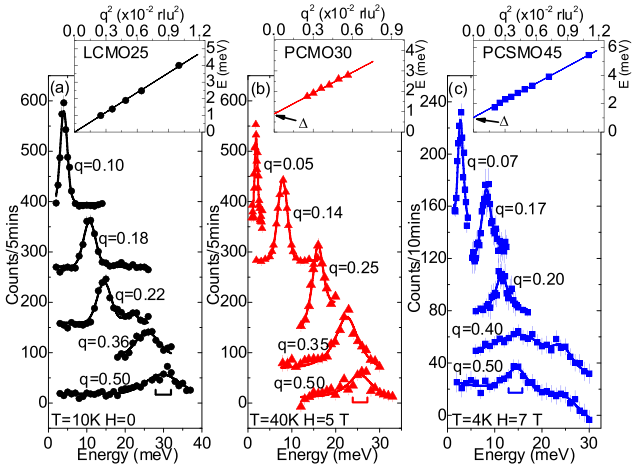

FIG. 2 (color online). The q-dependent spin-wave excitations in LCMO25 (a), PCMO30 (b), and PCSMO45 (c) at low temperatures. The data at different q's are incrementally shifted for clarity. The horizontal bars are the instrumental resolution and small shoulders around 25 meV in (c) are phonon scattering. E versus q^2 are plotted in the insets to determine D.

disorder and lattice distortions that control T_C's of different $x = 0.3$ manganites [17] have no effect on J_4/J_1, different from the expectations of the disorder effect theory [13]. These observations cannot be explained consistently by any current theory, thus suggesting that more than one mechanism is at play in determining the spin dynamical properties of the $A_{1-x}A'_xMnO_3$ manganites.

For this study, we used single crystals of $La_{0.75}Ca_{0.25}MnO_3$ (LCMO25), $Pr_{0.7}Ca_{0.3}MnO_3$ (PCMO30), and $Pr_{0.55}(Ca_{0.85}Sr_{0.15})_{0.45}MnO_3$ (PCSMO45) grown by the traveling solvent floating zone technique. We chose these samples because they represent a large span in carrier concentrations. While LCMO25 has a FM metallic ground state with $T_C = 191$ K [18], PCMO30 [19,20] and PCSMO45 [21] exhibit AFM insulating behavior at zero field but can be transformed into FM metallic phases by field cooling from room temperature (Fig. 1). Our neutron scattering experiments were performed on triple-axis spectrometers at the High-Flux Isotope Reactor (HFIR), Oak Ridge National Laboratory and the NIST Center for Neutron Research (NCNR). The momentum transfers $\vec{q} = (q_x, q_y, q_z)$ in units of Å^{-1} are at positions $(h, k, l) = (q_x a/2\pi, q_y b/2\pi, q_z c/2\pi)$ in reciprocal lattice units (rlu), where lattice parameters for LCMO25, PCMO30, and PCSMO45 are $a \approx b \approx c \approx 3.87$ Å, 3.856 Å, and 3.834 Å, respectively.

Figure 2 shows constant-q scans at representative wave vectors for LCMO25, PCMO30, and PCSMO45 along the [100] direction. The excitation peaks are sharp and resolution limited at low q, but become weak in intensity near the zone boundary. To obtain the strength of the average magnetic interaction, we analyze the low-q data using $E = \Delta + Dq^2$, where E is the spin-wave energy obtained from Gaussian fits, Δ is the field-induced Zeeman gap [20], and D is the spin-wave stiffness. The slopes of the E versus q^2 lines, shown in the insets of Fig. 2, yield D values of 150 ± 3, 145 ± 8, 152 ± 3 meV Å^2 for LCMO25, PCMO30, and PCSMO45, respectively. It is remarkable that all three samples exhibit very similar low-q behavior after they are driven into FM states either by temperature or by magnetic field. This suggests that the average kinetic energy derived from the hopping of the itinerant electrons between adjacent manganese ions is independent of carrier concentration.

To determine the evolution of magnetic excitations in $A_{1-x}A'_xMnO_3$ as a function of x, one must first understand the effect of on-site disorder arising from the mismatch between rare- and alkaline-earth-metal ions, as such disorder might induce anomalous spin dynamical behavior [13]. The disorder is characterized by $\sigma^2 = \sum_i (x_i r_i^2 - \bar{r}^2)$, where x_i is the fractional occupancies of A-site species, r_i and $\bar{r} = \sum_i x_i r_i$ are individual and averaged ionic radius, respectively, [22,23]. Figure 3(a) summarizes spin-wave dispersions along the [100] direction for a series of $A_{1-x}A'_xMnO_3$ with $x \approx 0.30$ [7–10,16], while the doping dependence of magnon excitations is shown in Fig. 3(b) [6,15]. The solid lines in the figure are phenomenological fits to the data using the Heisenberg Hamiltonian $E(\vec{q}) = \Delta + 2S[J(0) - \sum_j J_{ij} e^{i\vec{q}\cdot(\vec{R}_i - \vec{R}_j)}]$ with nearest-neighbor (J_1) and fourth-nearest-neighbor (J_4) exchange coupling. In the low-q limit, $E(q) = \Delta + 8\pi^2 S(J_1 + 4J_4)q^2$. This simple Hamiltonian gives a satisfactory description of the data, where J_4/J_1 measures the magnitude of the effective zone boundary magnon softening [15]. We note that our pre-

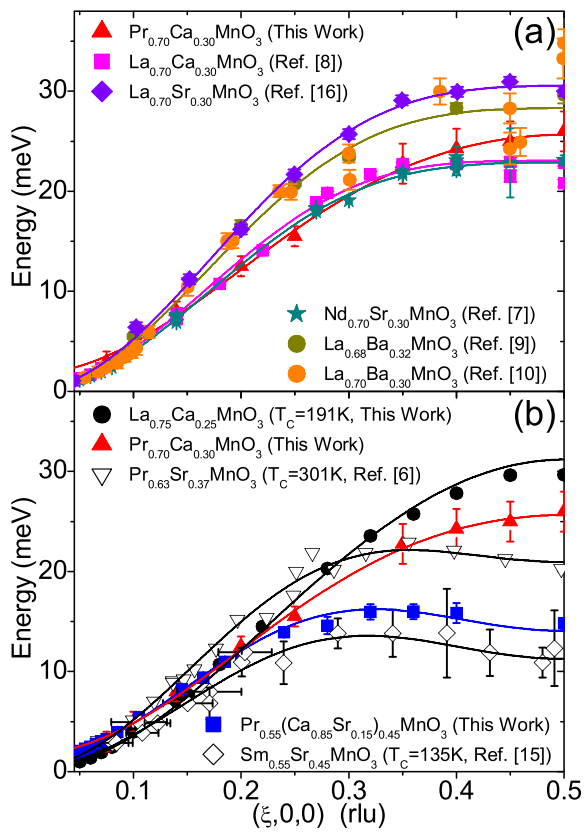

FIG. 3 (color online). (a) Spin-wave dispersion curves of various $A_{0.7}A'_{0.3}MnO_3$ manganites along the $[\xi, 0, 0]$ direction. (b) Dispersion curves for a series of $A_{1-x}A'_xMnO_3$ as a function of x. The solid lines are least-square fits using the Heisenberg model with J_1 and J_4.

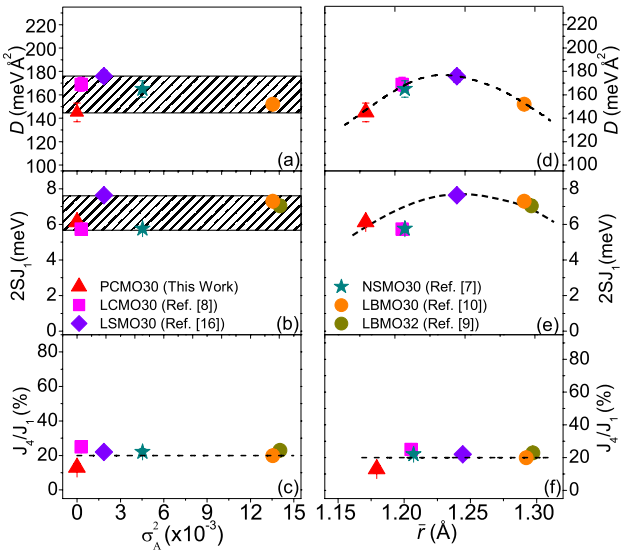

FIG. 4 (color online). The on-site disorder dependence of (a) the spin-wave stiffness D obtained from low-q excitations, (b) the coupling $2SJ_1$ and (c) the ratio of J_4/J_1. The average ionic radius dependence of (d) D, (e) $2SJ_1$, and (f) J_4/J_1. Dashed lines are guides to the eye.

vious experience [6] showed that J_2 and J_3 have small contributions to the total magnon dispersion.

We are now in a position to determine the effect of on-site disorder (σ^2) and average ionic size ($\bar{r}$) on spin-wave excitations of $A_{0.7}A'_{0.3}MnO_3$. Figs. 4(a)–4(c) show the σ^2 dependence of the spin-wave stiffness D, the nearest-neighbor exchange coupling J_1, and the ratio of J_4/J_1 in $A_{0.7}A'_{0.3}MnO_3$. With increasing disorder, the long-wavelength limit spin-wave stiffness shows no systematic trend but falls within a bandwidth of $D = 160 \pm 15$ meV Å^2 [Fig. 4(a)]. While such behavior at low q is not unexpected [7], numerical calculations suggest a significant zone boundary magnon softening with increasing disorder [13]. In other words, increasing σ^2 should have no effect on D but dramatically increase J_4/J_1. Surprisingly, Fig. 3(a) reveals no direct correlation between σ^2 and the zone boundary magnon energy; and Fig. 4(c) shows that J_4/J_1 is independent of σ^2. Therefore, the on-site disorder has no observable effect on zone boundary magnon softening.

In addition to inducing on-site disorder, replacing A by A' in $A_{0.7}A'_{0.3}MnO_3$ will also change the average ionic radius $\bar{r}$ and modify the length and angle of Mn-O-Mn bonds, thus leading to changes in effective transfer integrals between Mn ions or the bandwidth of the electrons [17]. Figs. 4(d)–4(f) show the $\bar{r}$ dependence of the spin-wave stiffness D, $2SJ_1$, and J_4/J_1. With increasing $\bar{r}$, D shows a parabolic curve within a small bandwidth. It increases from 160 meV Å^2 at $\bar{r} \sim 1.21$ Å for NSMO30 to 176 meV Å^2 at 1.25 Å for LSMO30, and then decreases to 152 meV Å^2 at 1.29 Å for LBMO30 [Fig. 4(d)]. The T_C's for NSMO30, LSMO30, and LBMO30 are 198 [7], 351 [16], and 350 K [10], respectively. Although increasing $\bar{r}$ leads to rapid changes in T_C, the kinetic energy (D) or bandwidth of the electrons only changes slightly [7,24]. Furthermore, J_4/J_1 is independent of $\bar{r}$ [Fig. 4(f)], thus indicating that the magnitude of the zone boundary magnon softening is independent of T_C and a general feature of the $A_{0.7}A'_{0.3}MnO_3$ manganites.

Assuming the effect of on-site disorder and ionic size is weakly doping dependent, we can then study how spin-wave excitations of $A_{1-x}A'_xMnO_3$ are modified as a function of x. For LSMO20, we used the stiffness value of $D = 166.8 \pm 1.51$ meV Å^2 obtained by high-resolution cold neutron triple axis at low q [16] because this value is more accurate than the earlier result of 120 meVÅ^2 obtained on a thermal triple axis [5]. Figure 5 summarizes the x dependence of D, $2SJ_1$, and J_4/J_1. Surprisingly, the spin-wave stiffness D is around 160 ± 15 meVÅ^2 and essentially unchanged for $0.2 \leq x \leq 0.45$ [Fig. 5(a)], while T_C varies from 305 K for LSMO20 [16] to 135 K for SSMO45 [15]. This is in sharp contrast to the expectation of all DE based models, where D increases with x [solid line in Fig. 5(a)] [3]. This also differs from a conventional ferromagnet, where T_C should be proportional to D. On the

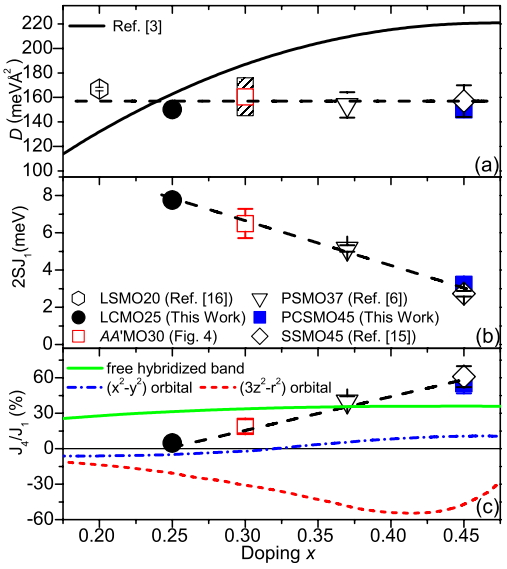

FIG. 5 (color online). Doping dependence of (a) spin-wave stiffness D, (b) nearest-neighbor exchange coupling J_1, and (c) ratio of J_4/J_1. Dashed lines are guides to the eye. The solid line in (a) is the prediction of Ref. [3]. The (green) solid, (blue) dash-dotted, and (red) dashed lines in (c) are calculations from different models in [15].

other hand, $2SJ_1$ decreases and J_4/J_1 increases, approximately linearly, with increasing x [dashed lines in Figs. 5(b) and 5(c)]. Therefore, J_4/J_1 does not exhibit a huge rise in magnitude for $x \geq 0.4$ as expected from the $(3z^2 - r^2)$-type orbital fluctuations (dashed line), nor does it follow the predictions of the $(x^2 - y^2)$-type orbital fluctuations (dash-dotted line) or free hybridized bands (solid line) shown in Fig. 5(c) [15].

Our systematic investigations in Figs. 4 and 5 put stringent constraints on microscopic theories of the zone boundary magnon softening. The possibility of on-site disorder-induced zone boundary softening is ruled out, as such a theory expects an enhanced softening with either increasing disorder or decreasing x [13], both contrary to the observation. Similarly, it is unclear how on-site Coulomb repulsion in a DE mechanism can explain the doping independent behavior of the spin-wave stiffness [3]. The magnon and $A_{1-x}A'_x$-site optical phonon coupling (crossing) scenario postulated for LCMO30 [8] also has difficulty in explaining the evolution of J_4/J_1, as the average $A_{1-x}A'_x$-site mass and frequencies of associated optical phonon modes do not vary dramatically from LCMO25 to SSMO45. If the large J_4/J_1 for $x = 0.45$ materials stems from fluctuations of the $(3z^2 - r^2)$ orbital, J_4/J_1 should have a spectacular doping dependence around $x = 0.4$ [15]. However, this is not observed. Furthermore, the $(3z^2 - r^2)$-type orbital fluctuations should have little or no effect on spin-wave softening at low carrier doping of $x = 0.25$ and 0.3. Therefore, it cannot be the origin of zone boundary magnon softening in $A_{1-x}A'_xMnO_3$ at all doping levels. Finally, we note that the free hybridized band model and $(x^2 - y^2)$ orbital fluctuation effects do not have the correct doping dependence for J_4/J_1 [Fig. 5(c)]. Although none of the current theories is capable of explaining the spin dynamics in the entire doping regime, it is possible that more than one effect determines the properties of spin excitations in manganites. For example, strong Coulomb repulsion in connection with the electron-phonon coupling can induce orbital polarization throughout the phase diagram. It is also known that chemical disorder can fundamentally modify the ground states of manganites [25] and be responsible for changes in spin dynamics [26]. To understand the evolution of spin dynamical behavior in $A_{1-x}A'_xMnO_3$, one must consider interactions among spin, charge, orbital, and lattice degrees of freedom.

This work is supported by the U.S. NSF No. DMR-0453804, DOE No. DE-FG02-05ER46202 and No. DE-AC05-00OR22725 with UT/Battelle LLC, and also by NSF No. DMR-0346826 and DOE No. DE-FG02-04ER46125. This work was performed under the U.S.–Japan Cooperative Program on Neutron Scattering.

*Electronic address: daip@ornl.gov

[1] C. Zener, Phys. Rev. **82**, 403 (1951).
[2] N. Furukawa, J. Phys. Soc. Jpn. **65**, 1174 (1996).
[3] D. I. Golosov, Phys. Rev. B **71**, 014428 (2005).
[4] T. G. Perring *et al.*, Phys. Rev. Lett. **77**, 711 (1996).
[5] Y. Endoh and K. Hirota, J. Phys. Soc. Jpn. **66**, 2264 (1997).
[6] H. Y. Hwang *et al.*, Phys. Rev. Lett. **80**, 1316 (1998).
[7] J. A. Fernandez-Baca *et al.*, Phys. Rev. Lett. **80**, 4012 (1998).
[8] Pengcheng Dai *et al.*, Phys. Rev. B **61**, 9553 (2000).
[9] S. N. Barilo *et al.*, J. Cryst. Growth **211**, 480 (2000).
[10] T. Chatterji *et al.*, Phys. Rev. B **66**, 214408 (2002).
[11] I. V. Solovyev and K. Terakura, Phys. Rev. Lett. **82**, 2959 (1999).
[12] N. Furukawa, J. Phys. Soc. Jpn. **68**, 2522 (1999).
[13] Y. Motome and N. Furukawa, Phys. Rev. B **71**, 014446 (2005).
[14] G. Khaliullin and R. Kilian, Phys. Rev. B **61**, 3494 (2000).
[15] Y. Endoh *et al.*, Phys. Rev. Lett. **94**, 017206 (2005).
[16] L. Vasiliu-Doloc *et al.*, J. Appl. Phys. **83**, 7342 (1998); The zone boundary data for LSMO30 are from work of J. W. Lynn *et al.* (unpublished).
[17] H. Y. Hwang *et al.*, Phys. Rev. Lett. **75**, 914 (1995).
[18] Pengcheng Dai *et al.*, Phys. Rev. B **64**, 224429 (2001).
[19] Y. Tomioka *et al.*, Phys. Rev. B **53**, R1689 (1996).
[20] J. A. Fernandez-Baca *et al.*, Phys. Rev. B **66**, 054434 (2002).
[21] Y. Tomioka and Y. Tokura, Phys. Rev. B **66**, 104416 (2002).
[22] L. M. Rodriguez-Martinez and J. P. Attfield, Phys. Rev. B **54**, R15 622 (1996).
[23] R. D. Shannon, Acta Crystallogr., Sect. A **32**, 751 (1976).
[24] P. G. Radaelli *et al.*, Phys. Rev. B **56**, 8265 (1997).
[25] D. Akahoshi *et al.*, Phys. Rev. Lett. **90**, 177203 (2003).
[26] T. J. Sato *et al.*, Phys. Rev. Lett. **93**, 267204 (2004).